



## Neuro-fuzzy modeling of Cu(II) and Cr(VI) adsorption from aqueous solution by wheat straw

Samia Rebouh<sup>a,\*</sup>, Mounir Bouhedda<sup>b</sup>, Salah Hanini<sup>a</sup>

<sup>a</sup>Laboratory of Biomaterials and Transport Phenomena (LBMP), University of Medea, Algeria, Avenue de l'ALN, Ain Dheb, Medea 26000, Algeria, Tel./Fax: +213 25785253; emails: [samrebouh@yahoo.fr](mailto:samrebouh@yahoo.fr) (S. Rebouh), [s\\_hanini2002@yahoo.fr](mailto:s_hanini2002@yahoo.fr) (S. Hanini)

<sup>b</sup>Laboratory of Advanced Electronic Systems (LSEA), University of Medea, Algeria, Nouveau pôle urbain, Medea 26000, Algeria, Tel. +213 25785080, Fax: +213 25785253; email: [bouhedda\\_mo@yahoo.fr](mailto:bouhedda_mo@yahoo.fr)

Received 14 February 2014; Accepted 13 January 2015

---

### ABSTRACT

In this study, an intelligent architecture-based neuro-fuzzy technique is used for the prediction of removal capacity of Cu(II) and Cr(VI) from aqueous solution using wheat straw as a biosorbent. The effect of operating parameters such as initial pH, temperature, contact time, straw particle size, and biosorbent's chemical treatment are studied to optimize the conditions for maximum removal capacity. A large database is collected from the different carried out experiments to allow the modelization of the adsorption process. This process could be described using classical mathematical models such as Langmuir, Freundlich, or a hybrid model. However, the learnt neuro-fuzzy architecture with the obtained experimental data presents good correlation ( $R^2 = 0.9999$ ) and shows that the intelligent model is able to predict accurately the removal amount of Cu(II) and Cr(VI) from wheat straw under different conditions.

*Keywords:* Adsorption; Chromium; Copper; Neuro-fuzzy; Prediction; Wheat straw

---

### 1. Introduction

The brutal and massive release of toxic residues in the environment led to the appearance of new risks, poorly evaluated for the ecosystem's balance. The degradation of the environment concerns all media—air, water, and soil—which is why caring for its protection is currently a major problem globally.

Conventional methods used for the effluents treatment [1–5]—including heavy metals removal—such as precipitation, redox, ion exchange, filtration, membrane processes, and evaporation are toxic, inefficient, and too expensive. They are applied for solutions at

low concentration [6–10]. A good alternative to these methods is the use of original biopolymers such as industrial and agricultural wastes [11–18], which have physicochemical properties to capture heavy metals via an adsorption mechanism.

Adsorption as a separation process has been widely used in environmental chemistry because of its relatively low cost, simplicity of design, and capacity for adsorbing a board range of pollutants at low concentration [19]. Many biosorbents have been tested for heavy metals removal because of their abundant availability and low cost. They have been investigated as potential adsorbents for removing these kinds of pollutants. The removal of copper ions from aqueous solution by hazelnut shell has been predicted [20]. The use of activated

---

\*Corresponding author.

carbon prepared from peanut shells for hexavalent chromium adsorption has been studied [21]. The adsorption of Cd(II), Zn(II), Cr(III), and Cr(VI) from aqueous solutions using hazelnut has been reported [22]. Removal of heavy metals ions by banana pith has been investigated [23]. The adsorption of Cu(II) from synthetic solutions using Irish sphagnum peat moss has been studied [24]. The removal of heavy metal ions from aqueous solutions by means of rice bran, soybean, and cottonseed hulls has been investigated [25]. The use of shells of lentil, wheat, and rice for Cu(II) removal from aqueous solutions has been studied [26]. The adsorption of Cu(II) from water, using decaying *Tamarix gallica* leaves, has been reported [27].

Many byproducts of agriculture have proved to be good low-cost adsorbents for the removal of both copper and chromium from water. Lignocellulosic residues include wood residues (sawdust and paper mill discards); agricultural residues include lignocellulosic agrowastes (sugarcane bagasse, wheat bran, wheat straw, corn stoves, etc.). Lignocellulosic wastes have an adsorption capacity comparable to other natural sorbents. They also have the advantage of very low or no cost, great availability, and simple operating processes. In fact, using lignocellulosic agrowastes as biosorbents, an added value is provided to products that otherwise would be considered as a waste [28].

Wheat straw is a natural non-toxic and abundant agricultural waste. It is a lignocellulosic material containing hydrolyzable groups that biodegrade into low molecular weight derivatives, so it can be used as a potential and safe biosorbent for heavy metals.

The removal capacity of a biosorbent that presents nonlinearities with the operating parameters has to be described accurately in order to get a correct predictive model [29]. There are two ways to do this. The first is to establish a mathematical model where the knowledge of chemistry, biology, and other sciences is used to describe a relationship, which is extremely difficult for the case treated in this work. The second way requires the use of experimental data to establish a relationship between output and inputs. This method is used in cases where the process involves extremely complex physical phenomena, or exhibits strong nonlinearities and dependence on various parameters. This second method is the most suitable one to be used for the problem treated in this paper.

Obtaining a mathematical model for a system can be rather complex and time consuming. This fact has led researches to adopt the neural and fuzzy techniques in modeling complex systems using the input–output data-sets. In fuzzy logic to model systems experience, human knowledge is used rather than rules. It is not always easy to infer experience and

human knowledge to the rules of a fuzzy logic system. Moreover, fuzzy parameters have to be optimized. Artificial neural networks (ANNs) can be advantageous because they provide an adjusting mechanism that can be used to optimize the fuzzy system. The combination of ANNs with fuzzy systems creates a new, robust model called Adaptive Neural Fuzzy Inference System (ANFIS) [30].

In recent years, many researchers have adopted fuzzy logic technique in the field of processes engineering. Fuzzy model of titration curve to pH processes control has been used [31]. A fuzzy control model for improving nitrogen removal, in order to optimize the anoxic/oxic step feeding activated sludge process, has been proposed [32]. Fuzzy modeling and simulation to lead removal using micellar-enhanced ultrafiltration have been performed [33]. The pressure swing adsorption process of propylene/propane using neuro-fuzzy modeling has been optimized [34].

ANFIS, which is a specific approach in neuro-fuzzy development that has shown significant promise in modeling nonlinear functions, can be a good alternative and can be used in this work. It learns features of the data-set and adjusts the system characteristics according to a given error criterion.

In this work, the adsorption of copper and chromium using the wheat straw, performed in batch experiments, was investigated. This agricultural waste, cultivated in the province of Medea in the north of Algeria, was chosen because of its abundance. Several studies have demonstrated the capacity of different lignocellulosic materials to adsorb and remove significant amounts of toxic metals from aqueous solutions, but few have studied the wheat straw as biosorbent. In this study, a chemical treatment has been carried out to improve the ability of the wheat straw to capture Cu(II) and Cr(VI) ions. In addition, the effect of various operational parameters such as initial pH, temperature, contact time, particle sizes, and metal ionic charge nature was explored.

The second aim of our investigation was to develop a neuro-fuzzy model able to predict Cu(II) and Cr(VI) removal efficiency by wheat straw. Furthermore, to evaluate the performance of the developed ANFIS model, three classic empirical models are considered for comparison: Langmuir, Freundlich, and Redlich–Peterson.

## 2. Materials and methods

### 2.1. Material

Wheat straw was washed with demineralized water, dried in open air for five days, then placed in

an oven at 60°C for three hours before being carefully cut with scissors, and then ground using an electric grinder. At this stage, impurities are eliminated, which allows water to diffuse into the pores. The powder of wheat straw is subjected to a particle size treatment and then separated into five diameter classes: <250 µm, >250 µm, >500 µm, >750 µm, and >850 µm. These fractions were subsequently immersed in deionized water, filtered for three hours, dried in open air for 24 h, and then placed in an oven at 60°C for three hours.

## 2.2. Adsorbent chemical treatment

The biosorbents were put under chemical treatments in order to activate their sites before putting them in contact with ionic solutions. They were divided into three categories, two of them are handled as follows: in the first batch, the sample is placed in contact with a solution (0.2 N) H<sub>2</sub>SO<sub>4</sub> for eight hours with continuous stirring (stirrer CTIP, Italy, 125 rounds/min), rinsed with deionized water until a pH value of 6.5 is reached (pH measured by pH meter), and dried at 60°C. The obtained biosorbent is called “H-sorbent”.

Half of H-sorbent quantity was immersed in a 0.25 g/L Ca(OH)<sub>2</sub> solution for eight hours with continuous stirring and rinsed with deionized water until pH 7 and dried at 60°C, the obtained biosorbent is called “Ca-sorbent”. The third untreated sample is called “NT-sorbent.”

## 2.3. Preparation of ion solutions

On the other hand, aqueous solutions of copper sulfate CuSO<sub>4</sub> and potassium dichromate K<sub>2</sub>Cr<sub>2</sub>O<sub>7</sub> are used as ion sources of Cu(II) and Cr(VI), respectively. The initial concentration of the ionic solution before being placed in contact with the biosorbent, is equal to 20 mg/L for copper and 11 mg/L for dichromate.

## 2.4. Adsorption experimental studies

### 2.4.1. Kinetic adsorption experiments

The adsorption of Cu(II) and Cr(VI) ions was studied in a batch process at room temperature  $T = 25^\circ\text{C}$ . Adsorption experiments are performed by putting a mass of about 250 mg of dry wheat straw in two flasks containing each one 250 ml of copper and chromium solutions buffered at pH 5. Samples were taken at selected times, 02.5, 05.0, 10.0, 15.0, 30.0, 45.0, and 60.0 min, and filtered for the analysis of the residual

metal concentration in solution by atomic absorption spectrophotometer (AA800, USA). Samples taken for analysis are not returned to the flask. Consequently, the adsorbed amount of ion per unit of wheat straw mass  $q_i$  (mg/g), at time  $t_i$  is calculated using following equation:

$$q_i = \frac{C_0V_0 - C_iV_{i-1}}{m} \quad (1)$$

where  $C_0$  and  $C_i$  (mg/L) are the Cu(II) or Cr(VI) initial concentration and concentration at time  $t_i$ , respectively;  $V_0$  (L) is the initial volume of ion solution;  $V_{i-1}$  is the volume in contact with wheat straw before taking the last sample, and  $m$  (g) is the mass of wheat straw added to the flask.

### 2.4.2. Effect of pH

Batch experiments were carried out at different pH values of 2.0, 2.5, 3.0, 3.5, 4.0, 4.5, and 5.0 at room temperature by shaking 250 mg of wheat straw particles size <250 µm with 250 ml of metal ion solution for an optimal time (optimized previously) at a fixed agitation speed of 150 rpm. pH adjustment was conducted in a pH meter using a 1 M HCl or 1 M NaOH solutions.

### 2.4.3. Effect of temperature

Experiments were performed by placing 250 mg of wheat straw particles size <250 µm in a series of flasks containing 250 ml of metal ion solution at pH 5. The flasks were agitated on a shaker at 150 rpm while keeping the temperature at 25, 30, 35, 40, 45, 50, 55, and 60°C. Samples were taken from each flask at selected times and filtered for the analysis.

### 2.4.4. Effect of straw particle size

Adsorption experiments were performed by shaking 250 ml of metal ion solution in a series of flasks containing separately six different particle sizes of wheat straw (<250 µm, >250 µm, >500 µm, >750 µm, >850 µm) buffered at pH 5. Samples were taken at a previously optimized time and filtered for the analysis of the residual metal concentration in solution.

### 2.4.5. Effect of chemical treatment

As cited before, wheat straw was activated using acidic and alkaline treatment. To evaluate the effect of

these treatments on the removal capacity of the lignocellulosic sorbent, three following forms were placed in a series of three flasks: untreated NT-adsorbent, H-adsorbent, and Ca-adsorbent. Since the pH has a significant influence on ionic strength, it has been judged interesting to carry out each series of flasks in a different pH (from 2 to 5).

## 2.5. Fuzzy modeling

### 2.5.1. Fuzzy inference system

Since the introduction of fuzzy sets theory by Zadeh in 1965, it has impressed upon a wide variety of disciplines and has become one of the most powerful techniques to modelize the behavior of complex multi-input nonlinear systems.

In the concept of fuzzy logic, numbers are assigned to linguistic variables to represent uncertainties; a fuzzy value represents the relationship between a vague or uncertain quantity  $x$  and a membership function  $\mu$ , which ranges between 0 and 1 [35]. The inference rule is an “if-then” rule, which has the general form “If  $x$  is  $A$  then  $y$  is  $C$ ”, where  $A$  and  $C$  are linguistic values defined by fuzzy sets in the universes of discourse of  $X$  and  $Y$ , respectively. The if-part is called the antecedent and the then-part is called the consequent of a rule.

The relation  $\mu_a(x)$  given by Eq. (2) is a fuzzy membership function, which defines the grade of membership of  $x$  in  $A$  [35]. The most commonly used forms of membership functions are triangular, trapezoidal, bell shape, Gaussian, or sigmoidal functions.

$$A = \{x, \mu_a(x)/x \in X\} \quad (2)$$

A fuzzy inference system, also known as fuzzy rule-based system or fuzzy model, is represented in Fig. 1 [36]. It is composed of four conventional blocks:

- (1) Knowledge base unit containing a number of fuzzy if-then rules that define the membership functions of the fuzzy sets used in the fuzzy rules.

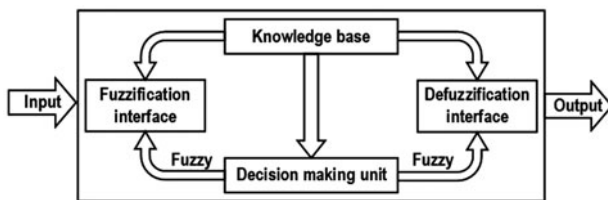


Fig. 1. Fuzzy inference system.

- (2) Decision-making unit which performs the inference operations on the rules.
- (3) Fuzzification interface which transforms the crisp inputs into degrees of match with linguistic values.
- (4) Defuzzification interface which transforms the fuzzy results of the inference into a crisp output.

### 2.5.2. Takagi–Sugeno fuzzy model

There are two types of fuzzy inference systems: Mamdani models [37] and Sugeno models [38]. The output membership functions of Mamdani models are fuzzy sets, which can incorporate linguistic information into the model, whereas the output membership functions of the models are either constant or linear functions of the input variables. Takagi–Sugeno (TS) are more suitable for adaptive modeling in combination with ANNs [39]. This kind of inference system is used in this work.

TS rules use functions of input variables as the rule consequent. For fuzzy modeling, a TS rule for three inputs ( $x_1$ ,  $x_2$ , and  $x_3$ ) and one output ( $y$ ) is given using following equation:

$$\text{if } x_1 \text{ is } A_1 \text{ and } x_2 \text{ is } A_2 \text{ and } x_3 \text{ is } A_3 \text{ then } y = f(x_1, x_2, x_3) \quad (3)$$

where  $A_1$ ,  $A_2$ , and  $A_3$  are fuzzy sets in the antecedent,  $y = f(x_1, x_2, x_3)$  is a crisp function in the consequent. Usually, the function  $f$  is a polynomial in the input variables  $x$  and  $y$ , but it can be any function as long as it can appropriately describe the output of the model within the fuzzy region specified by the antecedent of the rule. When  $f(x, y)$  is a first-order polynomial, the resulting fuzzy inference system is called a first-order Sugeno fuzzy model (Fig. 2), which was originally proposed in [37] and [38]. When  $f$  is a constant, a zero-order Sugeno fuzzy model is obtained.

### 2.5.3. ANFIS architecture

In this work, an ANFIS is going to be used as it's necessary to give a detailed description of the architecture. Fig. 3 shows the ANFIS architecture where the circular nodes represent fixed operations, whereas square nodes represent functions with parameters to be learnt. As shown in Fig. 3, ANFIS has five layers and the function of these layers can be explained briefly as follows [40].

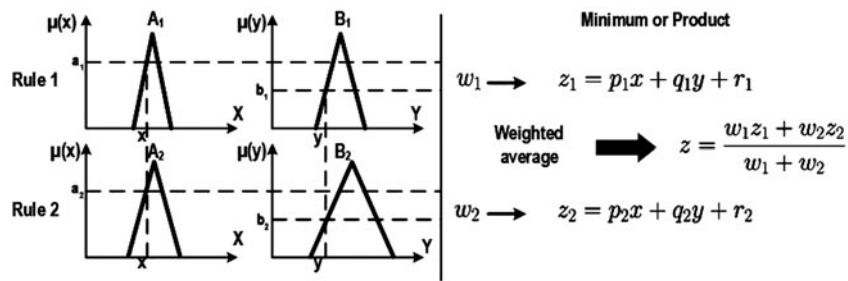


Fig. 2. First-order Sugeno fuzzy model.

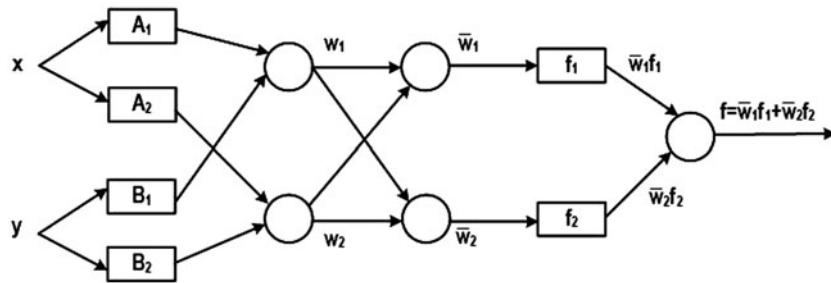


Fig. 3. ANFIS architecture.

Layer 1: In this layer where the fuzzification process takes place, every node is adaptive. Outputs of this layer form the membership values of the premise part.

The output of each node is given using following equation:

$$\begin{aligned} O_{1,i} &= \mu_{A_i}(x) \quad \text{for } i = 1, 2 \\ O_{1,i} &= \mu_{B_{i-2}}(y) \quad \text{for } i = 3, 4 \end{aligned} \tag{4}$$

So, the  $O_{1,i}(x)$  and  $O_{1,i}(y)$  are essentially the membership grade for  $x$  and  $y$ , respectively.

The membership functions could be triangular, trapezoidal, or any other function, but for illustration purposes, we will use the bell-shaped function given using following equation:

$$\mu_A(x) = \frac{1}{1 + \left| \frac{x-c_i}{a_i} \right|^{2b_i}} \tag{5}$$

where  $p_i, q_i, r_i$  are the parameters to be learnt, these are the premise parameters.

Layer 2: The nodes in this layer are fixed. Each node output represents a weight of the rule. Every node in this layer is fixed. This is where the  $t$ -norm is

used to “AND” membership grades. The following product is an example (Eq. (6)):

$$O_{2,i} = w_i = \mu_{A_i}(x)\mu_{B_i}(y) \quad \text{for } i = 1, 2 \tag{6}$$

Layer 3: The nodes are also fixed in this layer. The ratio of the  $i$ th rule’s firing weight to the sum of all rules weights is computed for the corresponding node. It contains fixed nodes that calculate the ratio of the firing strengths of the rules (Eq. (7)):

$$O_{3,i} = \bar{w}_i = \frac{w_i}{w_1 + w_2} \tag{7}$$

Layer 4: The nodes in this layer operate as a function block, whose parameters are adaptive and variables. They are the input values. The output of this layer forms TSK outputs.

The nodes in this layer are adaptive and perform the consequent of the rules (Eq. (8)):

$$O_{4,i} = \bar{w}_i f_i = \bar{w}_i(p_i x + q_i y + r_i) \tag{8}$$

The parameters in this layer ( $p_i, q_i, r_i$ ) are to be determined and are referred to as the consequent parameters.

Layer 5: It sums all the incoming signals and produces the output. There is a single node here, and it computes the overall output (Eq. (9)):

$$O_{5,i} = \sum_i \bar{w}_i f_i = \frac{\sum_i w_i f_i}{\sum_i w_i} \quad (9)$$

This is how, typically, the input vector is fed through the network layer by layer. We now consider how the ANFIS learns the premise and consequent parameters for the membership functions and the rules.

For ANFIS learning, there are a number of possible approaches, but we will discuss the hybrid-learning algorithm proposed by Jang et al. [41], which uses a combination of back-propagation and least squares estimation (LSE). It can be shown that for the network described, if the premise parameters are fixed the output is linear in the consequent parameters.

The total parameter set is split into two sets: the set of premise parameters ( $S_1$ ) that contains the parameters for all the chosen inputs membership functions, and the set of consequent parameters ( $S_2$ ) that contains the parameters of the output membership function.

So, ANFIS uses a two pass learning algorithms: the forward pass where  $S_1$  is unmodified and  $S_2$  is computed using an LSE algorithm, and the backward pass where  $S_2$  is unmodified and  $S_1$  is computed using a back-propagation algorithm. Therefore, the hybrid-learning algorithm uses a combination of the two mentioned algorithms to adapt the parameters in the adaptive network.

Model validation is an important step in the modelization phase. In practice, the ANFIS is validated with the data remaining for the test purpose. Eq. (10) gives the root mean square error (RMSE), which is the mean criterion used to evaluate the model performance [30].

$$\text{RMSE} = \sqrt{\frac{1}{N} \sum_{i=1}^N (y_i - \hat{y}_i)^2} \quad (10)$$

where  $N$  is the number of the tested data,  $y_i$  is the  $i$ th desired output, and  $\hat{y}_i$  is the  $i$ th predicted output from the model.

#### 2.5.4. ANFIS modeling setup

The developed ANFIS has six inputs corresponding to the operating parameters and one output corresponding to the adsorbent amount as illustrated by Fig. 4. Experimental data values are divided into two

parts, 90% of them are used for ANFIS identification and the remaining data are used to test the obtained ANFIS architecture. When using ANFIS toolbox of MATLAB, many approaches are tested by making changes on the type and number of input membership functions and the type of the output membership function. Table 1 gives the details of the best obtained results on the learning phase. To validate the obtained ANFIS model, 10 sets of parameters for both  $\text{Cu}^{2+}$  and  $\text{Cr}_2\text{O}_7^{2-}$  were tested with experimental data that are not used for ANFIS architecture identification. Table 2 shows accuracy less than  $3 \times 10^{-2}$  for the developed model in the prediction of the amount of adsorbed ions.

### 3. Results and discussion

#### 3.1. Adsorption experiments studies

##### 3.1.1. Kinetic adsorption

The removal efficiency as a function of contact time is shown in Fig. 5. It is evident from the figure that adsorption equilibrium was established in 15 min for Cu(II) and 30 min for Cr(VI). These times are taken as the adsorption equilibrium times for all other experiments. The adsorption process can be divided into two stages. The adsorption capacity increased rapidly in the first 15 min for the copper and in the first 30 min for the chromium, after which, no significant change was noted. This can be explained by the fact that ions have firstly occupied the available external sites on the adsorbent surface and then slowly diffused into the porous structure. A comparison between the ANFIS model prediction and the experiment data is shown in Fig. 5. A very good performance on prediction of experimental data was predicted using the ANFIS model.

Pseudo-first-order and pseudo-second-order models have been applied to find out the adsorption mechanism. The equation of Cu(II) and Cr(VI) kinetic models is expressed as follows:

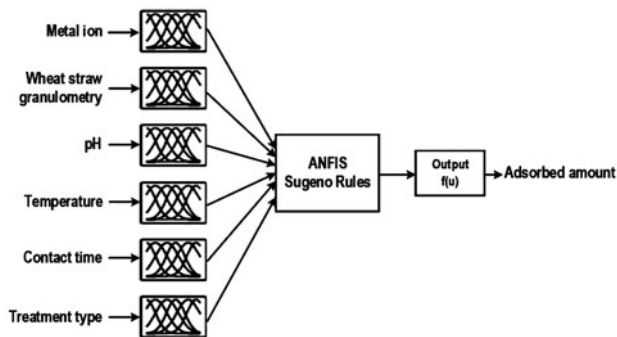


Fig. 4. ANFIS-developed architecture.



Table 1  
Best obtained results on the learning phase

Input	Input membership functions		Output membership function	Iterations	RMSE	$R^2$
	Type	Number				
Metal ion	Bell shape	2	linear	15	$6.7 \times 10^{-2}$	0.8918
Wheat straw granulometry	Bell shape	2				
pH	Bell shape	3				
Temperature	Bell shape	2				
Contact time	Bell shape	2				
Treatment	Bell shape	3				

The pseudo-first-order equation is given using following equation:

$$\frac{1}{q_t} = \frac{K_1}{q_e t} + \frac{1}{q_e} \quad (11)$$

where  $K_1$  is the pseudo-first-order rate constant ( $\text{min}^{-1}$ ) of adsorption,  $q_e$  and  $q_t$  (mg/g) are the amounts of metal ion adsorbed at equilibrium and at time  $t$  (min), respectively. The value of  $1/q_t$  is calculated from the experimental results and plotted against  $1/t$  ( $\text{min}^{-1}$ ).

The linear form of pseudo-second-order equation can be written as Eq. (12):

$$\frac{t}{q_t} = \frac{1}{K_2 q_e^2} + \frac{1}{q_e} t \quad (12)$$

where  $K_2$  is the pseudo-second-order rate constant of adsorption ( $\text{min}^{-1}$ ), the adsorption rate may be controlled by intraparticle diffusion or interaction steps. The kinetic parameters for adsorption of  $\text{Cu}^{2+}$  and  $\text{Cr}_2\text{O}_7^{2-}$  ions by the lignocellulosic material are shown in Table 3. The experimental  $q_e$  values are in agreement with the calculated values using pseudo-first-order and pseudo-second-order kinetics. Based on the obtained correlation coefficients ( $R^2$ ), the pseudo-second-order equation was the model that furthered the best fit for the experimental kinetic data, suggesting chemical adsorption as the rate-limiting step of the adsorption mechanism and no involvement of a mass transfer in solution [42].

### 3.1.2. Effect of pH on removal efficiency

The pH of the aqueous solution influences the chromium ionic form and the dissociation of active functional groups (hydroxyl  $-\text{OH}$  and carboxyl  $-\text{COOH}$ ) present on the lignocellulosic material in the

residues of wheat straw. The surface charge density depends on the pH of solution where the  $\text{H}^+$  concentration may react with the functional groups on a biosorbent surface. The pH effect on removal efficiency of copper and chromium is shown in Fig. 6. The functional groups of the lignocellulosic material treated by  $\text{CaOH}_2$  have higher affinity for hexavalent chromium than copper (since pH of adsorption study is in range of 2–5, so chromium is on  $\text{Cr}_2\text{O}_7^{2-}$  ion form). The removal efficiency is higher in acidic pH (at pH 2, removal capacity is 83.54%) and it decreases when pH increases. However,  $\text{Cu}^{2+}$  is more readily adsorbed by H-sorbent compared to other biosorbent forms in less-acidic pH (at pH 5 the removal capacity is 26.9%); here, the  $\text{Cu}^{2+}$  removal capacity increases when pH increases.

At low pH, the functional groups in the surface of the lignocellulosic material are protonated and restrict the approach of cationic species as the result of repulsive forces. As the pH increases, the degree of protonation decreases, and the functional groups become negatively charged ( $\text{pH} > \text{pK}_a$ ). From Fig. 6, it can be deduced that the obtained results using ANFIS model matches those obtained by the experimental.

Furthermore, the interpolated and extrapolated data are very significant; they fit perfectly with the experimental curve shape. We note, in this case, that the intelligent model can give each value so that the interpolation or the extrapolation is closer to the experiment result. However, in the empiric model, the interpolation is polynomial and the result is not always up to expectations.

### 3.1.3. Effect of the temperature

The effect of temperature on the adsorption of  $\text{Cu}^{2+}$  and  $\text{Cr}_2\text{O}_7^{2-}$  ion onto wheat straw lignocellulosic material was investigated. As shown in Fig. 7, the adsorption of the two metal ions decreases as the temperature increases from 25 to 60°C.

Table 2  
Comparison testing between experimental and predicted values

Straw wheat granulometry ( $\mu\text{m}$ )	Temperature ( $^{\circ}\text{C}$ )	pH	Treatment	Absorbent amount (g)	Initial ion concentration (mg/L)	Contact time (min)	Amount of adsorbed $\text{Cu}^{2+}$ (mg/g)			Amount of adsorbed $\text{Cr}_2\text{O}_7^{2-}$ (mg/g)			
							Experimental	ANFIS Predicted	Relative error (%)	Experimental	ANFIS predicted	Relative error (%)	
<250	35	4.0	H	250	20	10	2.9877	2.9784	0.3113	2.2248	2.2297	0.2202	
<250	35	2.5	NT	250	20	12	2.5163	2.5236	0.2901	1.4026	1.3964	0.4420	
<250	45	4.0	H	250	20	18	1.8079	1.8030	0.2710	3.4012	3.4080	0.1999	
<250	45	2.5	H	250	20	12	1.2440	1.2498	0.4662	0.3402	0.3372	0.8819	
<250	35	3.5	Ca	250	20	20	2.0377	2.0353	0.1178	2.7501	2.7538	0.1345	
<250	35	4.5	Ca	250	20	18	2.0841	2.0795	0.2207	2.4211	2.4112	0.4089	
<250	50	3.5	H	250	20	20	1.2320	1.2416	0.7792	2.2416	2.2420	0.0178	
<250	50	4.5	Ca	250	20	18	0.5321	0.5273	0.9020	0.9496	0.9417	0.8320	
<250	55	2.0	Ca	250	20	10	0.1039	0.1034	0.4813	0.0974	0.0983	0.9241	
<250	55	4.0	NT	250	20	12	1.9328	1.9351	0.1190	2.8474	2.8554	0.2810	
							$R^2 = 0.9999$	$R^2 = 0.9999$		$R^2 = 0.9999$			
							$\text{RMSE} = 5.9 \times 10^{-3}$	$\text{RMSE} = 6.0 \times 10^{-3}$		$\text{RMSE} = 6.0 \times 10^{-3}$			



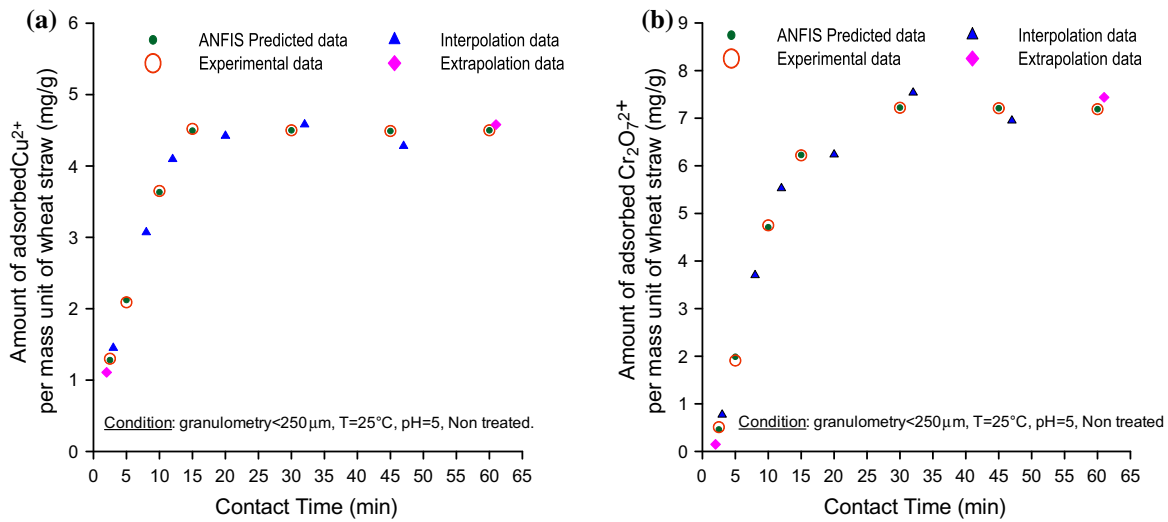


Fig. 5. Effect of contact time on the amount of adsorbed (a) copper and (b) chromium per mass unit of wheat straw and comparison between experimental and predicted data.

Table 3  
Kinetic parameters for Cu<sup>2+</sup> and Cr<sub>2</sub>O<sub>7</sub><sup>2-</sup> ions adsorption by wheat straw

Metal ion	First-order model			Second-order model		
	K <sub>1</sub> (min <sup>-1</sup> )	q <sub>e</sub> (mg/g)	R <sup>2</sup>	K <sub>2</sub> (min <sup>-1</sup> )	q <sub>e</sub> (mg/g)	R <sup>2</sup>
Cu <sup>2+</sup>	8.1699	5.8419	0.8862	0.0575	4.8482	0.9272
Cr <sub>2</sub> O <sub>7</sub> <sup>2-</sup>	31.7667	15.2097	0.8815	0.0107	8.8230	0.9450

Based on the fundamental concept of thermodynamics, and supposing that the reaction is in an isolated system, the system energy cannot be gained or lost and the entropy change is the only driving force. In order to gain insight into the mechanism involved in the adsorption, the following variations, standard Gibbs free energy ( $\Delta G_{ads}^\circ$ ), enthalpy ( $\Delta H_{ads}^\circ$ ), and entropy change ( $\Delta S_{ads}^\circ$ ), were determined from the slope and intercepted from the plots of  $\ln(K_C)$  vs.  $1/T$  (Fig. 7) according to Eqs. (13)–(15) [43].

$$K_C = \frac{X_e}{C_i - X_e} \tag{13}$$

where  $K_C$  is the equilibrium constant,  $X_e$  is the concentration of solute adsorbed on the wheat straw at equilibrium, mg/L,  $C_i$  is the initial ion concentration (mg/L).

$$\Delta G_{ads}^\circ = -RT \ln(K_C) \tag{14}$$

$$\ln(K_C) = \frac{\Delta S_{ads}^\circ}{R} - \frac{\Delta H_{ads}^\circ}{RT} \tag{15}$$

where  $R = 8.314 \text{ J/mol}$  and  $K$  is the gas constant.

The calculated values of thermodynamic parameters are shown in Table 4. As it can be seen, the negative values of  $\Delta G_{ads}^\circ$  for all ions under all conditions indicate the spontaneous nature of the adsorption. The negative ( $\Delta H_{ads}^\circ$ ) and ( $\Delta S_{ads}^\circ$ ) values means that the chemical exothermic process accompanied by a lowering in the entropy is due to the adsorption of the metal ions on the fiber surface, which is a common observation in most metal ions adsorption processes [42,43].

Once again, the model gives a good representation of experimental data and successfully predicts the effect of temperature on the copper and chromium adsorption amount. The interpolation and extrapolation show also a very good extension of the experimental data.

### 3.1.4. Effect of the wheat straw particle size

According to the results given in Fig. 8, the amount of metal adsorbed per unit mass of biosorbent is inversely proportional with the particle size of the biosorbent. This is due to the biosorbent–metal contact

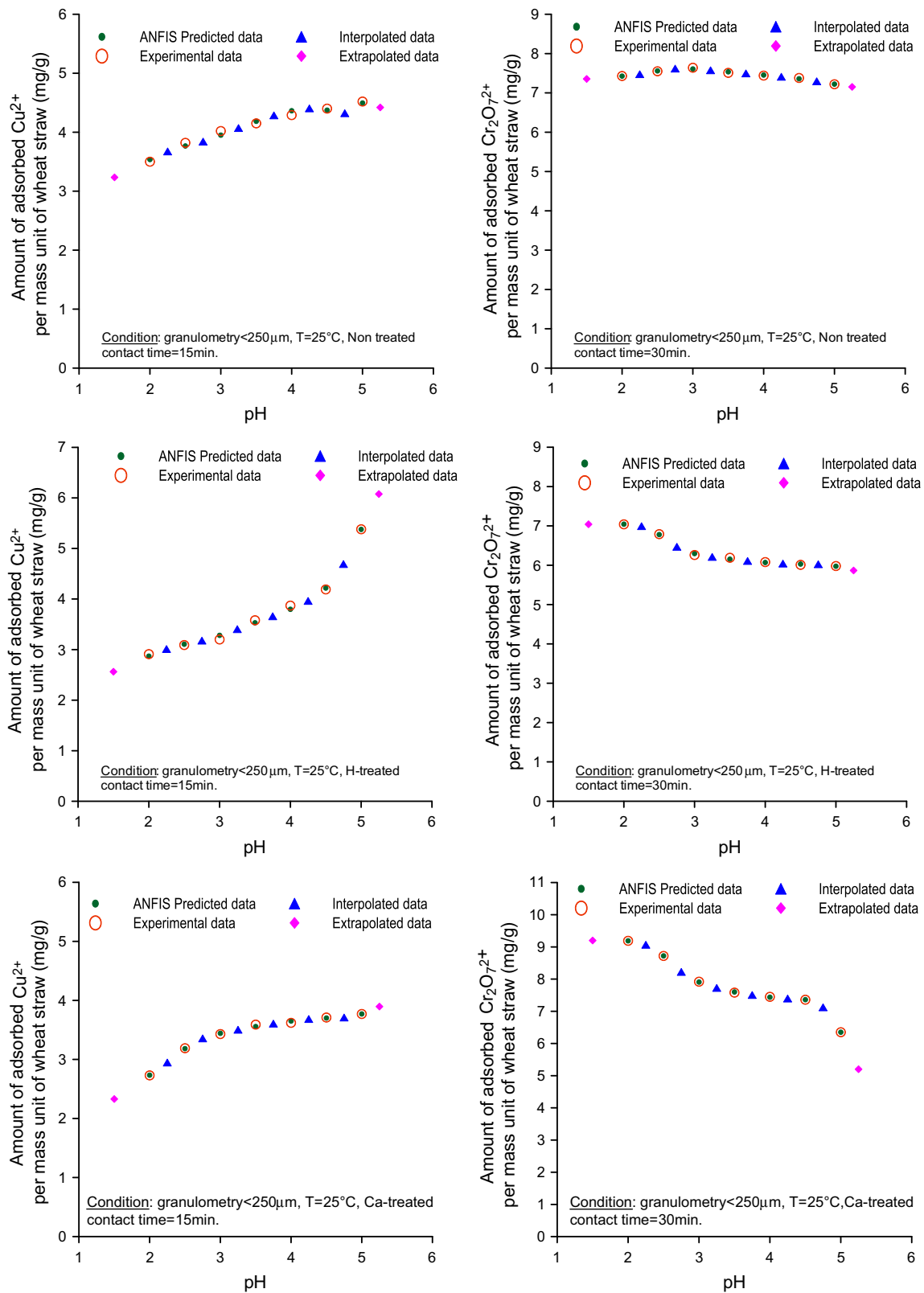


Fig. 6. Effect of pH on the amount of adsorbed copper and chromium per mass unit of wheat straw and comparison between experimental and predicted data.

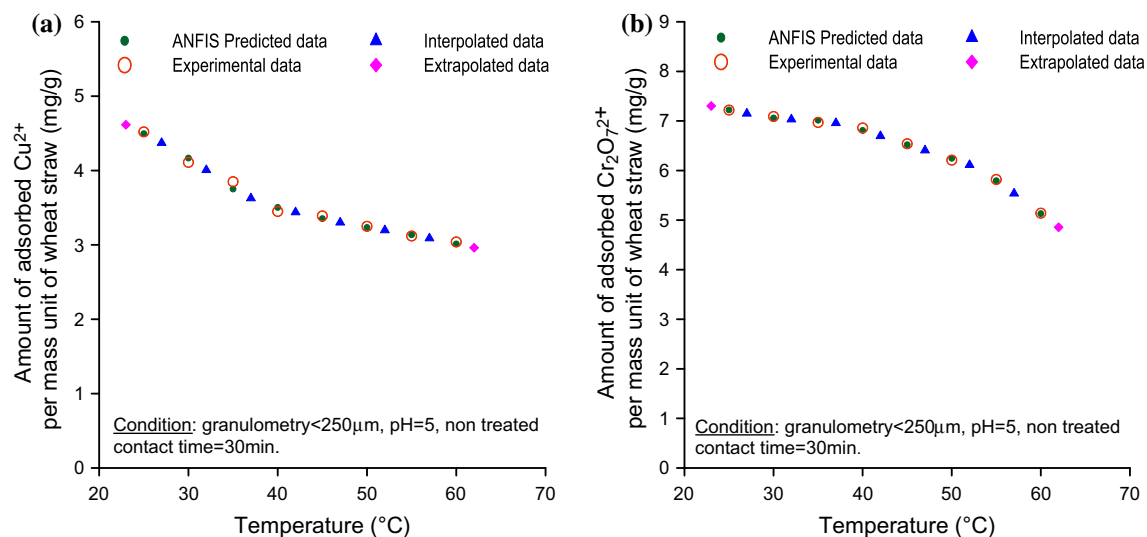


Fig. 7. Effect of the temperature on the amount of adsorbed (a) copper and (b) chromium per mass unit of wheat straw and comparison between experimental and predicted data.

Table 4  
Thermodynamic parameters for the adsorption of  $\text{Cu}^{2+}$  and  $\text{Cr}_2\text{O}_7^{2-}$  ions adsorption by wheat straw

Metal ion	$\Delta G_{\text{ads}}^{\circ}$ (kJ/mol) vs. Temperature (K)						$\Delta H_{\text{ads}}^{\circ}$ (kJ/mol)	$\Delta S_{\text{ads}}^{\circ}$ (J/mol K)
	298	303	308	313	323	333		
$\text{Cu}^{2+}$	0.720	0.649	0.609	0.541	0.520	0.495	-11.319	-49
$\text{Cr}_2\text{O}_7^{2-}$	4.732	4.567	4.427	4.312	3.480	2.428	-17.729	-53

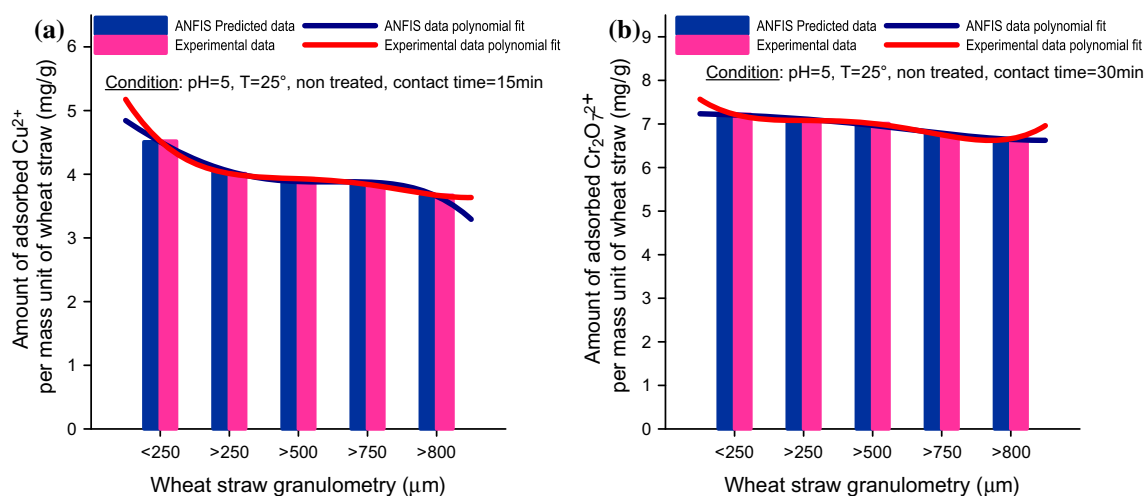


Fig. 8. Effect of wheat straw particle size on the amount of adsorbed (a) copper and (b) chromium per mass unit of wheat straw and comparison between experimental and predicted data.

surface. This surface increased due to the previously ground wheat straw that caused the release of active sites which were trapped in the structure. It is evident from Fig. 8 that the ANFIS model perfectly predicts the experimental data.

### 3.1.5. Effect of wheat straw chemical treatment

As shown in Fig. 9, lignocellulosic treatment with a weak acid promotes adsorption of  $\text{Cu}^{2+}$  cations under the protonation effect. Nevertheless, this surface protonation does not have a very significant effect, which is due to the lignocellulosic structure that hinders the activation of the OH groups present on the cellulose structure. On the other hand, the weak base gives the material a tendency to capture  $\text{Cr}_2\text{O}_7^{2-}$ . Once again, the ANFIS model matches the experimental data very well.

### 3.2. Mathematical models for adsorption isotherms

For the ion-biosorbent system, the adsorption isotherms at room temperature have been established with the adsorbed ion concentration in the solid phase (biosorbent) called  $C_{\text{ads}}$  (mg/g), as a function of the ion concentration in solution at equilibrium denoted  $C_{\text{eq}}$  (mg/L) solution, the term  $C_{\text{ads}}$  is given using following equation.

$$\frac{X}{M} = C_{\text{ads}} = \frac{(C_{\text{int}} - C_{\text{eq}})V}{m} \quad (16)$$

where  $C_{\text{int}}$  is the ion initial concentration (mg/L),  $C_{\text{eq}}$  is the ion concentration in solution at equilibrium

(mg/L),  $V$  is the ionic solution volume (L),  $m$  is the biosorbent mass (g).

The adsorption isotherms of copper and hexavalent chromium by the lignocellulosic material are given in Fig. 10. They have the same shape that corresponds to the isotherm model of type (I) given in the literature [44]. Since  $C_{\text{eq}}$  is given using following equation:

$$C_{\text{eq}} = C_{\text{int}} - C_{\text{sol}} \quad (17)$$

The isotherms show that when the concentration of copper decreases in the solution, it increases on the biosorbent surface (having an increasing and concave curve relative to the  $x$ -axis) until reaching a balance between the two phases liquid and solid, which corresponds to the saturation point. This effect is successfully predicted by ANFIS model where a similar histogram is found for both experimental and predicted data.

To investigate the adsorption capacity of Cu(II) and Cr(VI) on the biosorbent, mathematical models that correspond to the type I isotherm, namely, Langmuir, Freundlich, Redlich–Peterson, and hybrid isotherm, were applied.

#### 3.2.1. Langmuir isotherm model

When adsorption occurs in a single layer at sites—adsorption that can contain only one molecule per site (forming a monolayer) without interactions between the adsorbed molecules—it represents one of the best-known isothermal models (the Langmuir model),

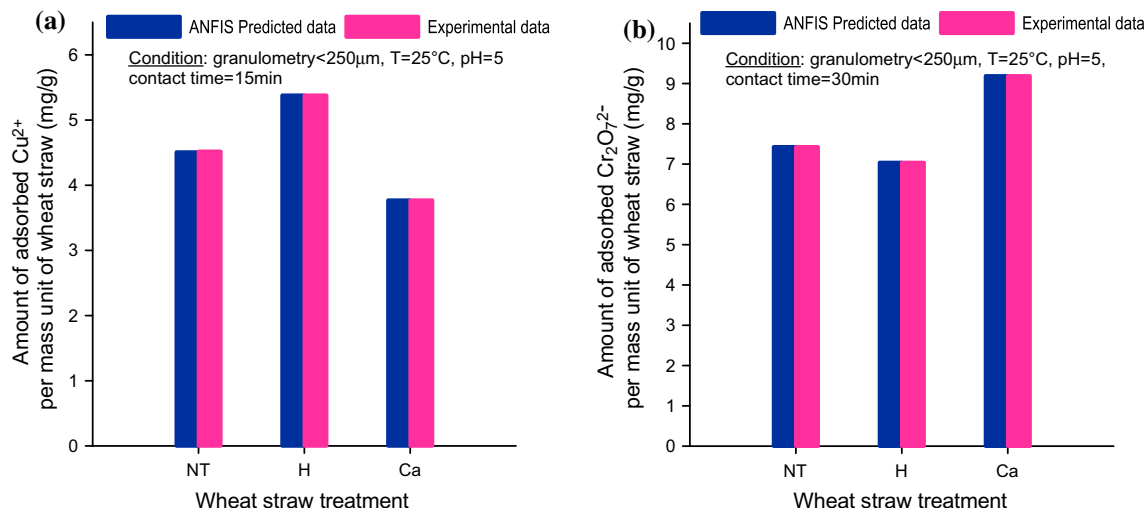


Fig. 9. Effect of wheat straw chemical treatment on the amount of adsorbed (a) copper and (b) chromium per mass unit of wheat straw and comparison between experimental and predicted data.

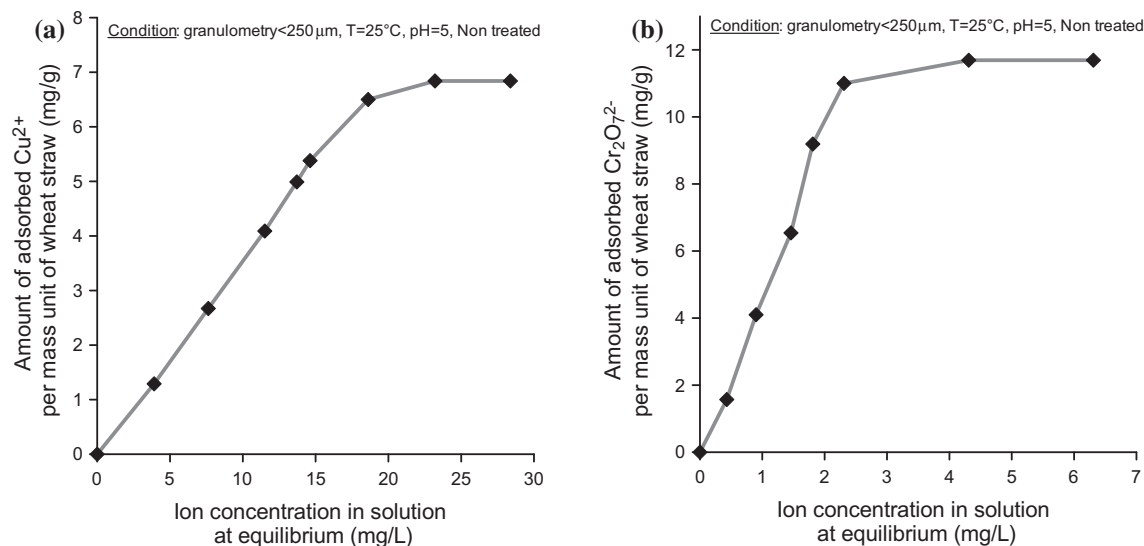


Fig. 10. Adsorption isotherm of (a)  $\text{Cu}^{2+}$  and (b)  $\text{Cr}_2\text{O}_7^{2-}$  into wheat straw.

whose expression is given using the following equation [44].

$$C_{\text{ads}} = \frac{K_L C_{\text{eq}}}{1 + b C_{\text{eq}}} \quad (18)$$

where  $C_{\text{ads}}$  is the amount of adsorbed ions per mass unit of biosorbent (mg/g),  $C_{\text{eq}}$  is the ion concentration in solution at equilibrium (mg/L),  $K_L$  is the Langmuir constant,  $C_{\text{max}} = \frac{K_L}{b}$  is the maximum amount of ions adsorbed on one gram of biosorbent.

### 3.2.2. Freundlich isotherm model

The Freundlich equation is well suited to describe the equilibrium in the aqueous phase. Its empirical formula is given using the following equation [42]:

$$\frac{X}{M} = C_{\text{ads}} = P C_{\text{eq}}^{\frac{1}{n}} \quad (19)$$

Langmuir model assumes that the biosorbent surface is homogeneous. However, the Freundlich isotherm is an indication of adsorption heterogeneity.

### 3.2.3. Redlich–Peterson isotherm model (hybrid isotherm)

Redlich–Peterson isotherm [45] is a hybrid featuring both Langmuir and Freundlich isotherms, which incorporates three parameters into an empirical equation [46]. The model has a linear relationship with

concentration in the numerator and an exponential function in the denominator [47] To represent adsorption equilibrium over a wide concentration range, such a model can be applied either in homogeneous or heterogeneous systems due to its versatility [48]. Typically, a minimization procedure is adopted in solving the equations by maximizing the correlation coefficient between the experimental data points and theoretical model predictions using Matlab programs [49]. In the limit, it approaches Freundlich isotherm model at high concentration and is in accordance with the low concentration limit of the ideal Langmuir condition [50]. The empirical formula of Redlich–Peterson isotherm model is given by the Eq. (20).

The results obtained from adsorption isotherms for  $\text{Cu}^{2+}$  and  $\text{Cr}_2\text{O}_7^{2-}$  using the wheat straw are shown in Table 5. The Langmuir isotherm had a better correlation ( $R^2 = 0.9442$ ) than both Freundlich and Redlich–Peterson models with the experimental data of the chromium adsorption. Homogenous distribution of active sites on lignocellulosical fiber surfaces could be the reason. However, for the copper adsorption, all the used models had shown a good correlation with the experimental data where  $R^2$  values are higher than 0.9442. It specifies the opportunity for simultaneous validity of multiple models [46].

$$C_{\text{ads}} = \frac{K_R C_{\text{eq}}}{1 + a_R C_{\text{eq}}^s} \quad (20)$$

Eq. (21) gives a better understanding of the adsorption mechanism of copper and chromium, another hybrid model that combines Langmuir and Freundlich models.

Table 5  
Parameters for the adsorption of  $\text{Cu}^{2+}$  and  $\text{Cr}_2\text{O}_7^{2-}$  ions by wheat straw according to different equilibrium models

Metal ion	Model													
	Langmuir isotherm model			Freundlich isotherm model			Redlich–Peterson isotherm model				Hybrid isotherm model			
	$K_L$ (L/mg)	$b$	$R^2$	$p$	$n$	$R^2$	$K_R$	$a_R$	$g$	$R^2$	$K_H$	$b_H$	$n_H$	$R^2$
$\text{Cu}^{2+}$	0.3891	0.0038	0.9442	0.4363	1.1238	0.9448	0.6529	0.5822	0.1989	0.9448	2.5723	0.1085	0.7800	0.9808
$\text{Cr}_2\text{O}_7^{2-}$	5.0216	0.4598	0.9482	4.2619	1.3319	0.8475	7.4920	0.7372	0.4155	0.8498	0.0016	0.1096	2.1100	0.8211

Table 6  
Adsorption capacity of various adsorbents as reported in the literature

	Samples	Optimum pH	Adsorbed amount (mg/g)	References
Copper	Carbon pecan shell	3.6	94.99	[51]
	Coir pith	4–5	10.22	[18]
	Peanut hulls	NA	10.16	[52]
	Orange peel	6–8	06.03	[53]
	Banana peel	6–8	04.76	[53]
	Wheat straw	5.0	05.38	Our study
	Cocoa shell	2.0	02.86	[54]
Chromium	Hazelnut shell	5–7	06.60	[55]
	Pine needles	2.0	05.36	[17]
	Wool	2.0	08.66	[17]
	Sawdust	6.0	03.3	[56]
	Coconut tree sawdust	3.0	03.46	[57]
	Wheat straw	2.0	09.19	Our study
	Sugar cane bagasse	2.0	13.4	[58]
	Walnut	3.5	22.18	[59]
	Hazelnut	3.5	22.99	[59]
	Almond	3.2	14.3	[59]

$$C_{\text{ads}} = \frac{K_H C_e^{\frac{1}{n_H}}}{1 + b_H C_e^{\frac{1}{n_H}}} \quad (21)$$

This three parameters model fits better with the copper adsorption experimental data than the three previous models ( $R^2 = 0.9808$ ). Nevertheless, it does not correlate with the chromium adsorption ( $R^2 = 0.8211$ ).

#### 4. Comparison of adsorption capacities with other adsorbents

In this study, it is shown that wheat straw has a good removal capacity for Cu(II) and Cr(VI): 5.38 and 9.19 mg/g, respectively. Literature data for adsorption capacity of Cu(II) and Cr(VI), along with data obtained in this research, are compared in Table 6.

#### 5. Conclusion

In this work, the wheat straw, an agricultural waste, has proved its efficiency as biosorbent material to remove metal ions from aqueous solutions. The adsorption capacity of this material was enhanced using two different treatments. The biosorbent acidic treatment promotes Cu(II) adsorption. However, the wheat straw that went through an alkaline treatment better adsorbed Cr(VI). The adsorption capacity of  $\text{Cu}^{2+}$  and  $\text{Cr}_2\text{O}_7^{2-}$  decreased with an increase in temperature, confirming the spontaneous nature of the adsorption, as it is found to be effective at lower temperatures ( $T = 25^\circ\text{C}$ ). As the functional groups charge depends on pH, the optimal pH values obtained for adsorption of Cr(VI) and Cu(II) are two and five, respectively. A reduced wheat straw particle size allows more surface contact between ion and lignocellulosical material, and therefore, a better adsorption

rate. Adsorption kinetic analysis showed that the mechanism of adsorption depends on the metal ion charge. Best adsorption capacity of the wheat straw is observed with  $\text{Cr}_2\text{O}_7^{2-}$  anion—where it reached 83.5% onto Ca-treated biosorbent at pH 2 at room temperature of  $T = 25^\circ\text{C}$ —while the maximum adsorption rate of  $\text{Cu}^{2+}$  is 26.9% obtained in the case of H-treated wheat straw at pH 5 at room temperature of  $T = 25^\circ\text{C}$ . The Langmuir isotherm model was a better fit for the copper adsorption data, compared to the Freundlich and Redlich–Peterson models. On the other hand, the three models represented the chromium adsorption process, well but a hybrid model combining Langmuir and Freundlich models was more suitable for the chromium experimental data. Only one neuro-fuzzy architecture was successfully used to estimate the adsorption of both Cu(II) and Cr(VI) ions by the wheat straw from aqueous solutions where the values of  $R^2$  and the mean square error were 0.9999 and 0.006, respectively. Consequently, the new architecture gives better modelization than the three mathematical models. It also presents a perfect model to estimate interpolated and extrapolated data. The new predictive intelligent model can be used elsewhere, saving time and experimental effort. Furthermore, it enhances and gives a better understanding of the adsorption processes behavior, where other parameter effects can be investigated, like ion strength or agitation speed. This work is demonstrative and can be extended to use neuro-fuzzy models for predicting the adsorption amount of other heavy metals, even for inorganic products like dyes and organic solvents and so, for more adsorbate/adsorbent combinations.

## References

- [1] A. Borém, F.R. Santos, D.E. Bowen, Understanding Biotechnology, first ed., Prentice Hall, Upper Saddle River, NJ, 2003.
- [2] Ullmann, Ullmann's Encyclopedia of Industrial Chemistry, CD-ROM, seventh ed., Wiley-VCH, Berlin, 2007.
- [3] H.C. Vogel, C.M. Todaro, Fermentation and Biochemical Engineering Handbook: Principles, Process Design, and Equipment, second ed., Noyes Publications, Westwood, NJ, 1997.
- [4] F. Meinck, H. Stooff, H.M. Kohlschütter, Les eaux résiduaires industrielles (Industrial Residual Waters), second ed., Masson, Paris, 1977.
- [5] D. Hendricks, Fundamentals of Water Treatment Unit Processes: Physical, Chemical, and Biological, CRC Press, New York, NY, 2011.
- [6] M.O. Adebajo, R.L. Frost, J.T. Klopogge, O. Carmody, S. Kokot, Porous materials for oil spill cleanup: A review of synthesis and absorbing properties, *J. Porous Mater.* 10(3) (2003) 159–170.
- [7] S. Babel, T.A. Kurniawan, Low-cost adsorbents for heavy metals uptake from contaminated water: A review, *J. Hazard. Mater.* 97(1–3) (2003) 219–243.
- [8] S.E. Bailey, T.J. Olin, R.M. Bricka, D.D. Adrian, A review of potentially low-cost sorbents for heavy metals, *Water Res.* 33(11) (1999) 2469–2479.
- [9] Y. Bal, K.E. Bal, A. Lallam, Removal of Bi(III) and Zn (II) by nonliving *Streptomyces rimosus* biomass from nitric solutions, *Eur. J. Miner. Process. Environ. Prot.* 3 (1) (2003) 42–48.
- [10] B. Kong, B. Tang, X. Liu, X. Zeng, H. Duan, S. Luo, W. Wei, Kinetic and equilibrium studies for the adsorption process of cadmium(II) and copper(II) onto *Pseudomonas aeruginosa* using square wave anodic stripping voltammetry method, *J. Hazard. Mater.* 167 (1–3) (2009) 455–460.
- [11] N. Angelova, D. Hunkeler, Rationalizing the design of polymeric biomaterials, *Trends Biotechnol.* 17(10) (1999) 409–421.
- [12] G. Cárdenas, P. Orlando, T. Edelio, Synthesis and applications of chitosan mercaptanes as heavy metal retention agent, *Int. J. Biol. Macromol.* 28(2) (2001) 167–174.
- [13] N. Chiron, R. Guilet, E. Deydier, Adsorption of Cu(II) and Pb(II) onto a grafted silica: Isotherms and kinetic models, *Water Res.* 37(13) (2003) 3079–3086.
- [14] L. Dupont, E. Guillon, J. Bouanda, J. Dumonceau, M. Aplincourt, EXAFS and XANES studies of retention of copper and lead by a lignocellulosic biomaterial, *Environ. Sci. Technol.* 36(23) (2002) 5062–5066.
- [15] S.O. Lesmana, N. Febriana, F.E. Soetaredjo, J. Sunarso, S. Ismadji, Studies on potential applications of biomass for the separation of heavy metals from water and wastewater, *Biochem. Eng. J.* 44(1) (2009) 19–41.
- [16] D. Feng, C. Aldrich, Adsorption of heavy metals by biomaterials derived from the marine alga *Ecklonia maxima*, *Hydrometallurgy* 73(1–2) (2004) 1–10.
- [17] M. Dakiky, M. Khamis, A. Manassra, M. Mer'eb, Selective adsorption of chromium(VI) in industrial wastewater using low-cost abundantly available adsorbents, *Adv. Environ. Res.* 6(4) (2002) 533–540.
- [18] K. Kadirvelu, K. Thamaraiselvi, C. Namasivayam, Removal of heavy metals from industrial wastewaters by adsorption onto activated carbon prepared from an agricultural solid waste, *Bioresour. Technol.* 76(1) (2001) 63–65.
- [19] A. Dong, J. Xie, W. Wang, L. Yu, Q. Liu, Y. Yin, A novel method for amino starch preparation and its adsorption for Cu(II) and Cr(VI), *J. Hazard. Mater.* 181(1–3) (2010) 448–454.
- [20] E. Demirbas, N. Dizge, M.T. Sulak, M. Kobya, Adsorption kinetics and equilibrium of copper from aqueous solutions using hazelnut shell activated carbon, *Chem. Eng. J.* 148(2–3) (2009) 480–487.
- [21] Z.A. AL-Othman, R. Ali, M. Naushad, Hexavalent chromium removal from aqueous medium by activated carbon prepared from peanut shell: Adsorption kinetics, equilibrium and thermodynamic studies, *Chem. Eng. J.* 184(1) (2012) 238–247.
- [22] G. Cimino, A. Passerini, G. Toscano, Removal of toxic cations and Cr(VI) from aqueous solution by hazelnut shell, *Water Res.* 34(11) (2000) 2955–2962.
- [23] K.S. Low, C.K. Lee, A.C. Leo, Removal of metals from electroplating wastes using banana pith, *Bioresour. Technol.* 51(2–3) (1995) 227–231.
- [24] Y.S. Ho, G. McKay, Sorption of dyes and copper ions onto biosorbents, *Process Biochem.* 38(7) (2003) 1047–1061.



- [25] W.E. Marshall, L.H. Wartelle, D.E. Boler, M.M. Johns, C.A. Toles, Enhanced metal adsorption by soybean hulls modified with citric acid, *Bioresour. Technol.* 69 (3) (1999) 263–268.
- [26] H. Aydın, Y. Bulut, Ç. Yerlikaya, Removal of copper (II) from aqueous solution by adsorption onto low-cost adsorbents, *J. Environ. Manage.* 87(1) (2008) 37–45.
- [27] F.R. Zaggout, Removal of copper from water by decaying *Tamrix gallica* leaves, *Asian J. Chem.* 13(2) (2001) 639–650.
- [28] Q. Yu, X. Zhuang, Q. Wang, W. Qi, X. Tan, Z. Yuan, Hydrolysis of sweet sorghum bagasse and eucalyptus wood chips with liquid hot water, *Bioresour. Technol.* 116 (2012) 220–225.
- [29] C. Gerente, V.K.C. Lee, P. Cloirec, G. McKay, Application of chitosan for the removal of metals from wastewaters by adsorption—Mechanisms and models review, *Crit. Rev. Environ. Sci. Technol.* 37(1) (2007) 41–127.
- [30] J.-S.R. Jang, ANFIS: Adaptive-network-based fuzzy inference system, *IEEE Trans. Syst., Man, Cybern., Syst.* 23(3) (1993) 665–685.
- [31] M. Reza Pishvaie, M. Shahrokhi, Control of pH processes using fuzzy modeling of titration curve, *Fuzzy Set. Syst.* 157(22) (2006) 2983–3006.
- [32] M.-Z. Huang, J.Q. Wan, Y.-W. Ma, W.-J. Li, X.-F. Sun, Y. Wan, A fast predicting neural fuzzy model for on-line estimation of nutrient dynamics in an anoxic/oxic process, *Bioresour. Technol.* 101(6) (2010) 1642–1651.
- [33] B. Rahmanian, M. Pakizeh, M. Esfandiyari, F. Heshmatnezhad, A. Maskooki, Fuzzy modeling and simulation for lead removal using micellar-enhanced ultrafiltration (MEUF), *J. Hazard. Mater.* 192(2) (2011) 585–592.
- [34] M. Khalighi, S. Farooq, I.A. Karimi, Optimizing the PSA process of propylene/propane using neuro-fuzzy modeling, *Comput. Aided Chem. Eng.* 31 (2012) 1336–1340.
- [35] L.A. Zadeh, Fuzzy sets, *Inform. Control* 8(3) (1965) 338–353.
- [36] M. Chadli, P. Borne, Multiple Models Approach in Automation: Takagi–Sugeno Fuzzy Systems, first ed., Wiley-ISTE, London, 2012.
- [37] E.H. Mamdani, S. Assilian, An experiment in linguistic synthesis with a fuzzy logic controller, *Int. J. Man Mach. Stud.* 7(1) (1975) 1–13.
- [38] T. Takagi, M. Sugeno, Fuzzy identification of systems and its applications to modeling and control, *IEEE Trans. Syst., Man, Cybern. B, Cybern.* 15(1) (1985) 116–132.
- [39] Z. Huang, J. Hahn, Fuzzy modeling of signal transduction networks, *Chem. Eng. Sci.* 64(9) (2009) 2044–2056.
- [40] J. Patel, R. Gianchandani, ANFIS Control for Robotic Manipulators: Adaptive Neuro Fuzzy Inference Systems for Intelligent Control, LAP LAMBERT Academic Publishing, Saarbrücken, 2011.
- [41] J.-S.R. Jang, C.-T. Sun, E. Mizutani, *Neuro-Fuzzy and Soft Computing: A Computational Approach to Learning and Machine Intelligence*, first ed., Prentice Hall, Upper Saddle River, NJ, 1997.
- [42] M. Monier, D.M. Ayad, Y. Wei, A.A. Sarhan, Preparation and characterization of magnetic chelating resin based on chitosan for adsorption of Cu(II), Co(II), and Ni(II) ions, *React. Funct. Polym.* 70(4) (2010) 257–266.
- [43] Z. Reddad, C. Gerente, Y. Andres, P. Le Cloirec, Adsorption of several metal ions onto a low-cost biosorbent: Kinetic and equilibrium studies, *Environ. Sci. Technol.* 36(9) (2002) 2067–2073.
- [44] M. Suzuki, *Adsorption Engineering*, Elsevier Science, New York, NY, 1990.
- [45] O. Redlich, D.L. Peterson, A useful adsorption isotherm, *J. Phys. Chem.* 63(6) (1959) 1024–1024.
- [46] R. Krishnaprasad, S.N. Srivastava, Sorption of distillery spent wash onto fly ash: Kinetics and mass transfer studies, *Chem. Eng. J.* 146(1) (2009) 90–97.
- [47] J.C.Y. Ng, W.H. Cheung, G. McKay, Equilibrium studies of the sorption of Cu(II) ions onto chitosan, *J. Colloid Interface Sci.* 255(1) (2002) 64–74.
- [48] F. Gimbert, N. Morin-Crini, F. Renault, P.-M. Badot, G. Crini, Adsorption isotherm models for dye removal by cationized starch-based material in a single component system: Error analysis, *J. Hazard. Mater.* 157(1) (2008) 34–46.
- [49] Y.C. Wong, Y.S. Szeto, W.H. Cheung, G. McKay, Adsorption of acid dyes on chitosan-equilibrium isotherm analysis, *Process Biochem.* 39(6) (2004) 693–702.
- [50] L. Jossens, J.M. Prausnitz, W. Fritz, E.U. Schlünder, A.L. Myers, Thermodynamics of multi-solute adsorption from dilute aqueous solutions, *Chem. Eng. Sci.* 33 (8) (1978) 1097–1106.
- [51] R.A. Shawabkeh, D.A. Rockstraw, R.K. Bhada, Copper and strontium adsorption by a novel carbon material manufactured from pecan shells, *Carbon* 40(5) (2002) 781–786.
- [52] P. Brown, I. Atly Jefcoat, D. Parrish, S. Gill, E. Graham, Evaluation of the adsorptive capacity of peanut hull pellets for heavy metals in solution, *Adv. Environ. Res.* 4(1) (2000) 19–29.
- [53] G. Annadurai, R.S. Juang, D.J. Lee, Adsorption of heavy metals from water using banana and orange peel, *Water Sci. Technol.* 47(1) (2003) 185–190.
- [54] N. Meunier, J. Laroulandie, J.F. Blais, R.D. Tyagi, Cocoa shells for heavy metal removal from acidic solutions, *Bioresour. Technol.* 90(3) (2003) 255–263.
- [55] Ö. Demirbaş, A. Karadağ, M. Alkan, M. Doğan, Removal of copper ions from aqueous solutions by hazelnut shell, *J. Hazard. Mater.* 153(1–2) (2008) 677–684.
- [56] H.C.P. Srivastava, R.P. Mathur, I. Mehrotra, Removal of chromium from industrial effluents by adsorption on sawdust, *Environ. Technol. Lett.* 7(1–2) (1986) 55–63.
- [57] K. Selvi, S. Pattabhi, K. Kadirvelu, Removal of Cr(VI) from aqueous solution by adsorption onto activated carbon, *Bioresour. Technol.* 80(1) (2001) 87–89.
- [58] D.C. Sharma, C.F. Forster, A preliminary examination into the adsorption of hexavalent chromium using low cost adsorbents, *Bioresour. Technol.* 47(3) (1994) 257–264.
- [59] E. Pehlivan, T. Altun, Biosorption of chromium(VI) ion from aqueous solutions using walnut, hazelnut and almond shell, *J. Hazard. Mater.* 155(1–2) (2008) 378–384.